27th EPS Conference on Contr. Fusion and Plasma Phys. Budapest, 12-16 June 2000 ECA Vol. **24B** *(2000) 93 -96*

Recent experiments on fast electron transport in solid materials: electron inhibition and jet production

D. Batani, A. Antonicci, F. Pisani, A. Bernardinello, E. Martinolli
Dipartimento di Fisica "G.Occhialini" and INFM, Università degli Studi di Milano-Bicocca, Via Emanueli 15, 20126 Milan, Italy e-mail: batani@mi.infn.it

M. Koenig, L. Gremillet, F. Amiranoff, S. Baton
LULI, CNRS-Ecole Polytechnique, 91128 Palaiseau, France

T. Hall, D. Scott
University of Essex, Colchester, UK

C. Rousseaux
CEA-Bruyères-le Châtel, France

P. Norreys, A. Djaoui
Rutherford Appleton Laboratory, Chilton, Didcot, UK

P. Fews
University of Bristol, UK

H. Bandulet, H. Pepin
INRS, Energie et Matériaux, J3X1S2 Varennes, Québec, Canada

1. Introduction

In the so called "fast ignition" approach to ICF [1,2] a short-pulse high-intensity laser beam generates a beam of relativistic electrons which propagates in the compressed pellet, loosing energy and starting fuel ignition. The study of electron propagation in dense matter is hence essential to the success of the scheme.
In this context it is important to consider the generation of electric fields at the target surface where the laser is focused. As a great number of electrons is accelerated inside the target, the charge separation generates a strong electric field which inhibits the propagation of the electrons. Bell et al. [3] demonstrated that electrons cannot travel into a target for more than

$$z_o = 3\ 10^{-3}\ T_{hot}^{\ 2}\ \sigma_6\ I_{17}^{\ -1}\ \mu m$$

where σ_6 is the material conductivity in unit $10^6\ \Omega^{-1}\ m^{-1}$, T_{hot} is the electron temperature in keV, and I_{17} is the absorbed laser intensity in units 10^{17} W cm^{-2}. In order to study the electric inhibition we experimentally compared the penetration of fast electrons in solids (metallic conductors and plastic insulators). Also, an efficient heating of the core requires the electron beam to remain collimated up to its final absorption zone, i.e. on a distance of several hundreds of microns. This can only be achieved through the pinching effect of the beam-driven magnetic field competing with multiple scattering. This was studied with a time resolved shadowgraphy technique.

2. Experimental set-up

The experiments were performed with the LULI 100 TW laser based on chirped pulse amplification (CPA). A 350 fs (FWHM) 0.53 μm laser pulse with an energy up to 10 J was focused by a *f* /3 off-axis parabola at normal incidence onto the target, as shown in Fig.1, up to an incident laser intensity of the order of 10^{19} W/cm^2. Metals and insulator targets were used to show the importance of electric field inhibition. After the propagation layer (Al or CH), the fast electrons reach two layers of fluorescent materials (20 μm of Mo and 20 μm of

Pd) where they produce K_α photons. These are detected by a CCD camera used in single shot mode to allow spectroscopic analysis. A fourth 50 μm plastic layer on the rear side of the target avoided any spurious K_α emission. By changing the thickness of the propagation layer it was possible to obtain the penetration depth of fast electrons in the given material (plastic or aluminium).
In order to assure the same interaction conditions, even in the case of plastic targets the first layer was made of 1.2 μm Al. Hence any difference in experimental K_α yield was only due to differences in electron propagation through the solid materials, and not to a different rate or temperature of the produced fast electrons.

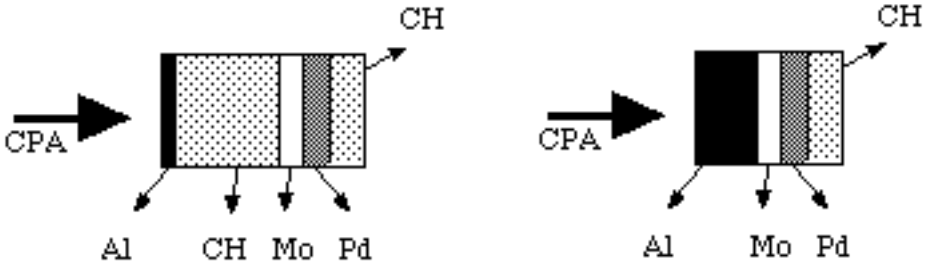

Fig. 1: Principle of the electron penetration experiment conducted at LULI

Alternatively, the laser was focused onto a 500 μm-wide edge of a fused silica plate. Each target was coated with a 10 μm Al foil, enough to prevent any transmission of the laser light. Moreover, frequency-doubling of the laser beam allowed a contrast ratio better than 10^8:1. A probe beam at 1.057 μm allowed a 2-D transverse imaging (shadowgraphy) of the target, with spatial and time resolutions respectively of the order of 5 μm and 600 fs. The region ionised up to a fraction of the critical density of 1.057 μm light becomes opaque to the probe. By varying the time delay between the probe and the main beam, it was possible to analyse the ionisation dynamics occurring within the glass slab.

3. Penetration Results

We realised two series of shots in which the laser intensity was changed by varying the focusing conditions. In the first, the focal spot diameter was about 30 μm and the intensity was 1-2 10^{18} W/cm^2, while in the second one the spot was less than 10 μm and the intensity 1-2 10^{19} W/cm^2. By comparing the predictions of Monte Carlo simulations and the experimental ratio of K_α yield of palladium and molybdenum as a function of the target thickness, we obtained the temperature of fast electron in the two cases: respectively about 180 keV and 400 keV in agreement with Beg's law [4]:

$$T_{hot} = 100\ (I_{17}\ \lambda^2)^{1/3}\ \text{keV}$$

where the laser intensity is in unit 10^{17} W/cm^2.
Fig. 2 shows the experimental Mo K_α emission as a function of the crossed thickness (in μm) for both plastic and aluminium targets for the high intensity case (1-2 10^{19} W/cm^2). An exponential fits to the results, gives the value for penetration: 263±49 for Al and 165±25 μm (experimental). Computer simulations based on collisional models instead yielded 256±16 μm and 717±36 μm respectively (assuming a 400 keV temperature). We see how the numerical value for Al is compatible with the experimental result, while in the case of plastic, there is a large discrepancy, showing a strong inhibition of penetration. A similar situation is found in the low intensity case. Moreover we see that, by decreasing the laser intensity (and hence the electron temperature) the penetration in plastic increases (being 205±80 μm) a surprising result which cannot be explained on the basis of collisional models.
In order to understand the results, one must consider electric field effects. Again, according to the model by Bell *et al*. the response of the target strongly depends on material conductivity.

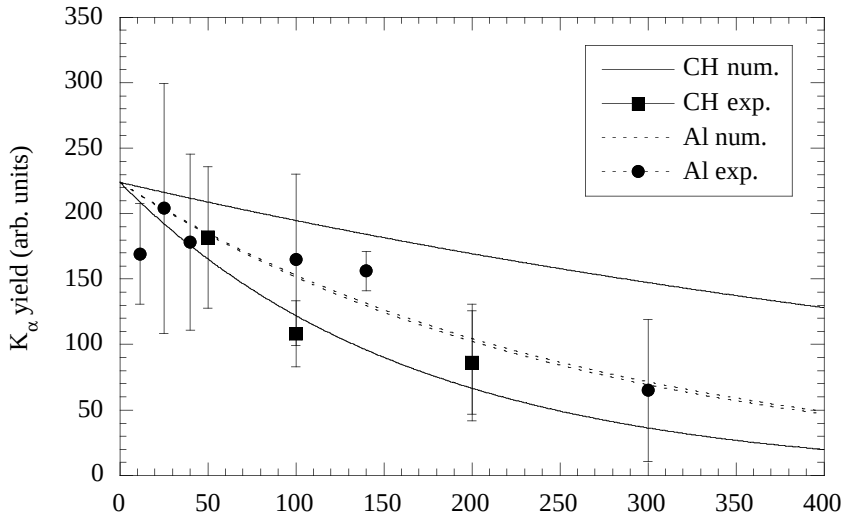

Fig. 2: Results at LULI in the high intensity case (T_{hot} = 400 keV):experimental and numerical K_α yield vs. target thickness in μm, and interpolation (exp(-R/R_0))

Our Al results imply $z_0 >> R_{coll}$ which is possible thanks to the high conductivity of Al. The situation is more complex with CH targets. A phase transition from insulator to conductor which produces free electrons available for the neutralising return current is essential to explain the observed penetration in plastic, even if some inhibition remains. Such phase transition is due both to heating of the target induced by fast electrons and to electric breakdown of the material. Although no models allow to calculate the conductivity of plastic for the temperatures we are interested in, we can infer that electric field effects will remain more important in the case of CH targets. Especially, the heating of the target will have opposite effects on Al and CH conductivity, the first being reduced with time (but keeping quite high values), while the second one increases starting practically from zero.
Despite the large error bars, a purely collisional explanation must be ruled out in plastic, since it implies an non-realistically low fast electron temperature of about 80 keV. This would be in complete disagreement with our Al results (the temperature must be the same!), and with published scaling laws.

4. Shadowgraphy Results

In this experiment the high-intensity short-pulse laser beam interacted with fused silica solid targets. Shadowgraphy was used as diagnostics of electron propagation, with a time resolution due to the duration of the probe beam of some 400 fs. The probe beam was absorbed where electrons induced ionisation of fused silica, producing dark regions in the images. These were taken varying the time delay between the main beam and the probe, allowing the velocity of electrons to be measured.
The shadowgraphic images of the target at three successive times are presented in Fig. 3. We can clearly see narrow (~20 μm) well-collimated long jets originating from the focal spot. Their length corresponds to a velocity very close to the velocity of light. Also visible, if less surprising, is the shape of a roughly isotropic cloud centered on the focal spot and expanding at a velocity roughly about c/2. Due to the 10 μm Al coating we used in this case, and the high contrast ratio of the laser pulse, we can arguably rule out the presence of any laser light within the target and thus assume that the only processes to be looked upon are due to fast electrons or hard X-rays. These latter have been ruled out by firing onto targets with a vacuum gap. Because of electric inhibition, this completely stops the fast electrons but it would not stop hard X-rays. In our experiments, the cloud and the jets completely disappeared, showing that these are really jets of relativistic electrons.
The observation of filamented hot electron structures obviously points to the role of self-generated magnetic fields. It has long been known that the interplay of magnetic focusing and collisionless pressure effects may result in a self-guiding regime in tenuous plasmas.

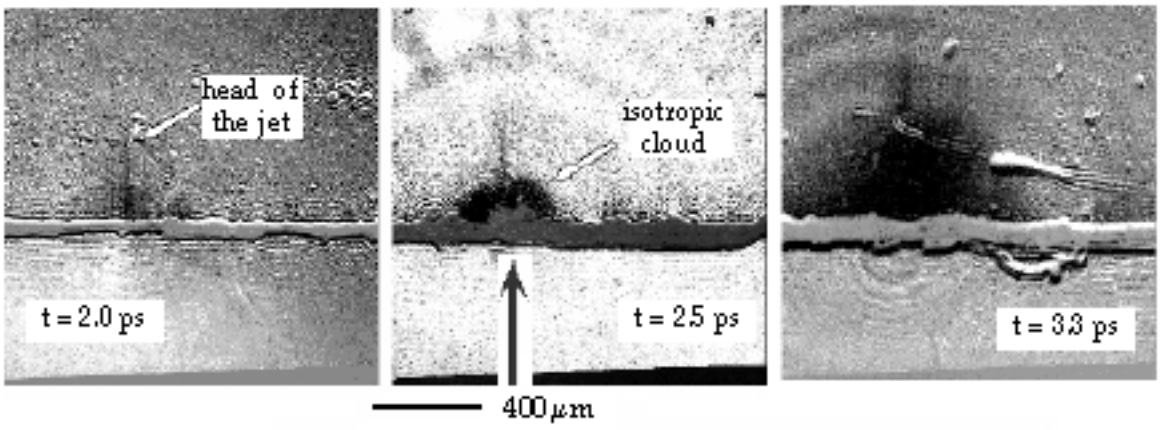

Fig. 3: Shadowgraphy images. The arrow shows the direction of the laser pulse.

In the case of solid-density targets, the first numerical predictions of such large-scale (up to 250 μm) collimated transport were obtained by Davies *et al.* [5]. We also point out that the return current is also very important to the propagation of the jets being crucial for a stable magnetic field-assisted regime, since the incident fast current largely exceeds the well-known Alfven limit [6].
The origin of the jets, and of the isotropic cloud, must still be fully understood. Due to the high target resistivity, electrons are not able to penetrate unless they ionise the background material producing free electrons available for the return current. This process is likely to take place on small localised regions, possibly connected to the non-homogeneous shape of the focal spot (characterised by the presence of laser hot spots). Once a low-resistivity channel has been created, electrons will tend to flow inside it, further increasing the local heating and reducing the resistivity. This mechanism, predicted by Haines several years ago, is know as electrothermal instability [7] and may play an important role in the formation of the jets which are then sustained by the strong magnetic fields.

5. Conclusions

We showed that in Al the large number of background electrons can neutralise the electric field in an effective way, while in plastic the electric response of matter is less important, which leads to an inhibition in the propagation. From a theoretically basis we do not exclude an influence of electric field inhibition in Al too. Anyway, this falls within our experimental error bars and is far less important. In any case, a proper analysis of the results of the propagation of electrons must take into account of the combination of collisions and electric effects.
The shadowgraphy experiment confirmed the ability of relativistic laser pulse-produced fast electrons to propagate in a collimated way over long distances into solid-density targets. Along with this dramatic feature, another regime of ultra fast energy transport, seemingly related to collisional electron propagation, has been observed. Among the fast ignitor-related issues that remain to be addressed is an explanation for this dual electron behaviour and an assessment of the dominant process as regards the heating efficiency.

Acknowledgements.

The experiments described in this work have been performed at LULI, supported by the E.U. Programme "Access to Large Scale Facilities" (Contract No. RBFMGECT950044).

References.

[1] M.Tabak, *et al.*, Phys. Plasmas, **1**, 1626-1634 (1994).
[2] S.Atzeni, Jpn. J. Appl. Phys. **34**, 1980 (1995).
[3] A.Bell *et al*., Plasma Phys. Control. Fusion, 39, 653-659 (1997).
[4] F.Beg *et al*., Phys. Plasmas, **4**, 447-457 (1997).
[5] J. R. Davies *et al*., Phys. Rev. Lett. E **56**, 7193 (1997).
[6] S. Humphries, Charged Particle Beams (Wiley Interscience, New York, 1990).
[7] M. G. Haines, Phys. Rev. Lett. **47**, 917 (1981).